ACS APPLIED MATERIALS & INTERFACES

Research Article

www.acsami.org

# The Development of Novel Nexar Block Copolymer/Ultem Composite Membranes for C2−C4 Alcohols Dehydration via Pervaporation

Jian Zuo,[†] Gui Min Shi,[†] Shawn Wei,[‡] and Tai-Shung Chung*[,†]

[†]Department of Chemical & Biomolecular Engineering, National University of Singapore, 4 Engineering Drive 4, Singapore 117576

[‡]Kraton Polymers, LLC, 15710 John F. Kennedy Boulevard, Suite 300, Houston, Texas 77032, United States

**ABSTRACT:** Novel composite membranes comprising sulfonated styrenic Nexar pentablock copolymers were developed by dip-coating on poly(ether imide) hollow fibers for pervaporation dehydration of C2−C4 alcohols. The advantages of using block copolymers as the selective layer are (1) their effectiveness to synergize the physicochemical properties of different chemical and structural moieties and (2) tunable nanoscale morphology and nanostructure via molecular engineering. To achieve high-performance composite membranes, the effects of coating time, ion exchange capacity (IEC) of the copolymer, and solvent systems for coating were investigated. It is revealed that a minimum coating time of 30 s is needed for the formation of a continuous and less-defective top layer. A higher IEC value results in a membrane with a higher flux and lower separation factor because of enhanced hydrophilicity and stretched chain conformation. Moreover, the composite membranes prepared from hexane/ethanol mixtures show higher separation factors and lower fluxes than those from the hexane solvent owing to microdomain segregation induced by ethanol and a smooth and dense top selective layer. These hypotheses were verified by atomic force microscopy and positron annihilation spectroscopy. The newly developed composite membranes demonstrate impressive separation performance with fluxes exceeding 2 kg/m$^2$ h and separation factors more than 200 for isopropyl alcohol and *n*-butanol dehydration from 85/15 wt % alcohol/water feed mixtures at 50 °C.

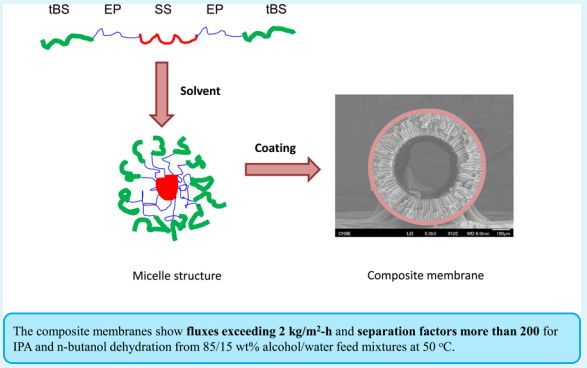


**KEYWORDS:** *block copolymer, composite membrane, alcohols, dehydration, pervaporation*

## 1. INTRODUCTION

Pervaporation is a promising separation technology for alcohol−water mixtures owing to the advantages of energy efficiency, environmental benignity, and simplicity in operation.[1−6] The successful development of suitable membranes is the cornerstone for a prosperous pervaporation process. Traditionally, hydrophilic polymers, such as poly(vinyl alcohol) (PVA), poly(acrylic acid) (PAA), chitosan, and sodium alginate, have been used to fabricate alcohol dehydration membranes.[7−9] However, these materials have poor mechanical stability in water due to excessive swelling, resulting in a significant decrease in separation efficiency. To circumvent the swelling issue, cross-linking or blending have often been utilized as two convenient methods.[10,11] Nevertheless, cross-linking modification may not be desirable since it not only reduces the permeation flux but also introduces an additional treatment step to the membrane fabrication, which prolongs the production procedure and increases the cost.

On the other hand, blending polymers may combine the advantages of different materials. Yoshikawa et al. have studied the gelatin/Torlon blended membrane for isopropyl alcohol (IPA) dehydration, and they reported a much enhanced separation performance than the individual neat membranes.[12,13] However, the blending method faces the challenge of immiscibility between different polymers, which may cause phase separation and narrow its applications. To synergize the strengths of different materials and improve the separation performance, membrane scientists have tried other approaches to integrate different components into one membrane, such as using organic linkers[14] or fabricating block copolymers.[15]

Block copolymers are a class of polymers that chemically embrace different structural and functional moieties into one polymer. Thus, these copolymers may possess desirable properties from different structural and functional moieties, while eliminating the phase separation problem as in many blended membranes. Because of these unique advantages, block copolymers have been considered as the dream materials for membrane fabrication for many years, yet the exploration of their full potential is by far not enough.[16] One of the first block copolymer membranes was tested for gas permeation by Odani et al. in 1975.[17] Since then the application of block copolymers has been extended to pervaporation. Boddeker et al. studied a polyether-block-amide (Pebax) membrane for pervaporation separation of aqueous phenolic solutions and alcohol solutions.

Received: May 26, 2014
Accepted: July 2, 2014
Published: July 2, 2014

  

Pebax demonstrated good separation efficiency toward organic solvents.[18,19] Recently, Buonomenna et al. investigated a poly(styrene-*b*-butadiene-*b*-styrene) (SBS) membrane for selective ethanol transport and examined the effect of nanoscale morphology of the block copolymer on the separation performance.[20] By controlling the nanostructure of the copolymer membrane, the overall separation performance can be largely changed. Hence, one can molecularly design the nanopores and membrane morphology by manipulating the chemical structure of each block and membrane formation conditions. This special property offers block copolymers infinite opportunities in molecular engineering and nanoscale designing.

Other than organic selective block copolymers, there are also a few studies on water-selective copolymers. Ray and his coworkers tested several commercial and self-synthesized block copolymers for the dehydration or organic compounds, such as acetic acid, tetrahydrofuran, and so on.[21,22] However, the report of using block copolymers for alcohol dehydration is rather limited.[23,24] Mandal and Pangarkar employed some acrylonitrile-based copolymer membranes for 1-methoxy-2-propanol dehydration and achieved good selectivity toward water.[24] Therefore, the possibility of applying block copolymers for alcohol dehydration should not be overlooked, and further research is necessary to explore their huge potentials.

In this study, a sulfonated styrenic pentablock copolymer, namely, Nexar polymer, is chosen for C2−C4 alcohol dehydration for its good water transport properties as demonstrated in other studies.[25,26] Therefore, the copolymer may potentially have a high selectivity and permeability toward water over alcohols. In addition, different chemical blocks in the copolymer provide different functions and contribute to the favorable physicochemical properties of the material: (1) Good mechanical stability and chain flexibility provided by the two *tert*-butylstyrene (*t*BS) end blocks and the two ethylene-*co*-propylene (EP) blocks, respectively.[27] (2) Formation of water transport channels owing to the middle sulfonated styrene (SS) block;[28] although the apparent contact angle may be in the hydrophobic range due to other blocks, these water transport channels may still be advantageous for the permeability. (3) Tunable ion exchange capacity (IEC) values depending on the degree of sulfonation. (4) Designable nanoscale morphology due to the incompatibility of different blocks in Nexar polymer that may lead to microdomain segregation under different solvents and form various nanostructures and morphologies. Studies have shown that Nexar polymer forms micelles in selective solvents such as cyclohexane and hexane, while it forms a lamellar state in some others such as chloroform.[29−31] Hence, all these properties offer great potential to design high-performance Nexar membranes for pervaporation applications.

Therefore, we aim to develop novel composite membranes by coating the Nexar polymer on poly(ether imide) hollow fiber substrates for alcohol dehydration. First, the effect of coating time on pervaporation performance of the resultant membranes is examined. Then, the nanostructures of the block copolymer are molecularly controlled by applying different solvent mixtures to achieve a good separation performance. The morphologies of formed composite membranes are investigated, and the changes in nanostructures are characterized. Subsequently, the effect of copolymer IEC values on the surface property of the composite membranes is studied. Lastly, the newly developed membranes are employed for C2−C4 alcohol dehydration to demonstrate their capability for pervaporation dehydration. This study may provide useful insights in designing and applying block copolymers for high-performance pervaporation membranes through molecular engineering and nanostructure manipulating of the copolymers.

## 2. EXPERIMENTAL SECTION

**2.1. Materials.** The Nexar pentablock copolymers with IEC values of 1.0, 1.5, and 2.0 (milli-equivalents of sulfonic acid per gram of dry polymer, meq/g) were provided by Kraton Polymers. The chemical structure is shown in Figure 1. Analytic-grade hexane and ethanol

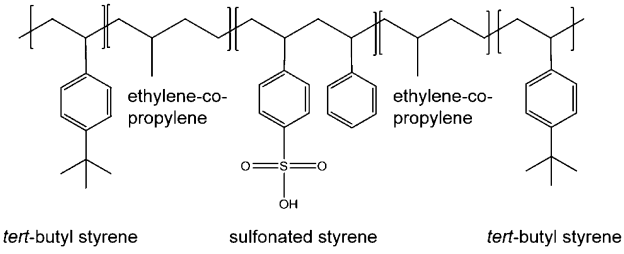


**Figure 1.** Chemical structure of the Nexar pentablock copolymer.

supplied by Merck were used to prepare the coating solutions. A commercial polymer Ultem 1010 supplied by the former GE plastics was used as the substrate material for the composite membranes. *N*-methyl-2-pyrrolidone (NMP) purchased from Merck was utilized as the solvent for hollow fiber spinning. Analytic-grade IPA and *n*-butanol used in the experiments were purchased from Merck.

**2.2. Spinning of Hollow Fiber Substrates.** Microporous Ultem hollow fibers were prepared in our lab as the substrate for composite membranes. A dope solution of Ultem/NMP/ethanol with the weight ratio of 23/72/5 was prepared to obtain a homogeneous mixture. The solution was then allowed to degas for 1 d before being transferred into an ISCO syringe pump. The mixture of NMP/*n*-butanol 95/5 (w/w) was used as the bore fluid to create a delayed demixing at the inner surface of hollow fibers. The dope solution and bore fluid were simultaneously extruded out of the spinneret orifice at the flow rates of 5 mL/min and 2 mL/min, respectively, and the nascent fiber was led into a water coagulation tank with an air gap of 5 cm and a take-up speed of 15 m/min. The collected fibers were immersed in a water bath for 3 d to remove the residual NMP. Subsequently, the fibers were cut into pieces of 25 cm in length and solvent exchanged in methanol followed by hexane three times each and then dried in air for usage. The detailed spinning procedures were described elsewhere.[32,33]

**2.3. Fabrication of Nexar Copolymer/Ultem Composite Membranes.** To fabricate composite membranes, 2 wt % Nexar copolymer coating solutions were first prepared by dissolving the copolymers with IEC values of 1.0, 1.5, and 2.0 in hexane. For some copolymers with an IEC value of 2.0, hexane/ethanol mixtures were also used to prepare the 2 wt % coating solutions as shown in Table 1.

**Table 1. Fabrication Conditions of Nexar Copolymer/Ultem® Composite Membranes**

| substrate | copolymer IEC value | solvent (wt %) for the copolymer | copolymer conc. (wt %) | coating time |
|---|---|---|---|---|
| Ultem fiber | 2.0 | hexane (100) | 2 | 10 s; 30 s; 1 min; 10 min |
| | | hexane/ethanol (80/20) | 2 | 30 s |
| | | hexane/ethanol (70/30) | 2 | 30 s |
| Ultem fiber | 1.5 | hexane (100) | 2 | 30 s |
| Ultem fiber | 1.0 | hexane (100) | 2 | 30 s |

Before carrying out dip coating on the outer surface of Ultem hollow fiber substrates, one end of the fibers was sealed by epoxy to prevent the coating solution flowing into the lumen side. Then, each time one fiber was vertically dipped into the preprepared solution with the sealed end heading downward for a designated time at room temperature. About 20 cm of the fiber was allowed to immerse in the solution, while the upper end was hung on a strain. Since the fiber is rigid and straight, there is no additional weight tied to the bottom. After the coating, the nascent composite membrane was hung up in air for 1 d under the ambient condition to allow the solvent to evaporate before usage. It might be a concern that gravity may affect the thickness of the membrane along the fiber length. This is especially true for continuous coating or very long hollow fiber substrates. However, for lab-scale coating in this study, the hollow fiber length is relatively short (25 cm). The effect of gravity may be negligible. In addition, because the coating layer is thin (in nanometer range), the interaction between the copolymer and polymer substrate would restrict the gravitational flow of top layer. Therefore, the membrane thickness should be relatively uniform.

**2.4. Characterizations.** Field emission scanning electron microscopy (FESEM JEOL JSM-6700LV) was used to observe the morphologies of the Ultem hollow fiber substrates as well as the composite membranes. The FESEM samples were prepared by fracturing the predried hollow fiber in liquid nitrogen and coated with platinum using a JEOL JFC-1200 ion sputtering device.

To investigate the changes in the interchain spacing of composite membranes prepared from different Nexar copolymer IEC values, a wide-angle X-ray diffraction (GADDS WXRD system, Bruker D8 advanced diffractometer) was performed. The measurement covered a scan range of $2\theta$ = 2.0 to 33.5° with a Ni-filtered Cu K$\alpha$ radiation at a wavelength $\lambda$ = 1.54 Å. The average chain spacing can be interpreted as $d$-spacing, which was determined based on Bragg's law.

$$n\lambda = 2d \sin\theta \tag{1}$$

where $n$ is an integral number (1, 2, 3, ...), $\lambda$ is the X-ray wavelength, $d$ is the dimension spacing, and $\theta$ is the diffraction angle. To study the surface hydrophilicity of membranes from different IEC values, the water contact angle was measured by a Sigma 701 Tensiometer from KSV Instruments Limited.

Slow beam positron annihilation spectroscopy (PAS) experiments were carried out to study the variation in free volume and depth profile of several predried composite membranes. Doppler broadening energy spectroscopy (DBES), one of the PAS spectrometers, was used to qualitatively investigate the free volume differences of the Nexar copolymer selective layers from different conditions and IEC values. A variable monoenergy slow positron beam was used to generate the DBES spectra as a function of positron incident energy (0−30 keV). An HP Ge detector (EG&G Ortec. with 35% efficiency and energy resolution of 1.5 at 511 keV peak) was used to collect the spectra data. One of the characteristic parameters of DBES spectra, namely, the $S$ parameter, defined as the ratio of the integrated counts at the central part of the annihilation $\gamma$ photo line to the total counts, was employed in this study as a qualitative measurement of the free volume in polymeric membranes.[34,35]

To understand the sorption properties of the Nexar copolymer to the three alcohols, namely, ethanol, IPA, and butanol, dense Nexar films were prepared and used for vapor sorption studies. A lab-scale kinetic sorption setup was utilized to measure the vapor sorption characteristics. The detailed schematic diagram and procedure can be found elsewhere.[36] The Nexar film samples were dried under vacuum, weighed by a microbalance, cut into small pieces of about 10 mg, and hung on a quartz spring in the sorption chamber. The solvent vapor was then generated from a 2 L liquid vessel by nitrogen at 50 °C. The evolution of quartz spring length was monitored with the aid of a Basler camera during sorption tests, and the sorption amount was calculated by the weight gain as follows:

$$\text{sorption(g/g membrane)} = \frac{(M_s - M_o)}{M_o} \tag{2}$$

where $M_o$ and $M_s$ are the membrane weights at initial state and sorption equilibrium, respectively.

The swelling tendency of the Nexar copolymer in three alcohols was also tested. First, the dense Nexar films were dried under vacuum and cut into small pieces of about 20 mm in length. Then, one piece of sample was sandwiched by two glass plates and immersed in one of the alcohol solutions. The exact membrane lengths before and after swelling were measured by a caliper. The degree of swelling was determined by the following equation:

$$\textit{extension}\% = \frac{L_2 - L_1}{L_1} \times 100\% \tag{3}$$

where $L_1$ and $L_2$ are the lengths of the membrane before and after swelling, respectively.

**2.5. Pervaporation Experiments.** The pervaporation setup for hollow fiber membranes has been depicted in Jiang's work.[37] A 2 L feed solution of alcohol/water 85/15 wt % mixture was circulated through the shell side of the hollow fiber with a flow rate of 30 L/h. The lumen side of the hollow fiber was the permeate side and was always under vacuum below 2 mbar. The variation of the feed concentration was less than 1 wt % during the entire experiment and hence can be considered as constant because of the large feed quantity compared with the permeate sample. The feed temperature was controlled at 50 °C with a circulating heating bath. The system was conditioned for 2 h to ensure that the membrane was stabilized before collecting the permeate samples, which was condensed in a cold trap immersed in liquid nitrogen and collected at a time interval of 1 h. The mass of the collected sample was weighed by a Mettler Toledo balance. The compositions of the feed and permeate samples were determined by a Hewlet-Packard GC7890 with an HP-INNOWAX column (packed with cross-linked polyethylene glycol) and a thermal conductivity detector (TCD). At least three permeate samples were collected, and the average pervaporation performance was reported.

Flux ($J$) and separation factor ($\alpha$) were calculated by the following equations:

$$J = \frac{Q}{At} \tag{4}$$

$$\alpha_{w/a} = \frac{Y_w/Y_a}{X_w/X_a} \tag{5}$$

where $Q$ is the total mass that permeates through the effective membrane area $A$ over the operation time $t$. Subscripts $w$ and $a$ refer to the components water and alcohol, while $Y$ and $X$ are the weight fractions of one component in the permeate and the feed side, respectively.

The fluxes and separation factors of some membranes were converted to permeance and selectivity to decouple the effect of driving force. First, the feed fugacity ($f_i$) was calculated by the following equation:

$$f_i = x_i \gamma_i P_i^{sat} \tag{6}$$

where $x_i$ is the mole fractional of component $i$ in the feed and $\gamma_i$ is the activity coefficient calculated by the Wilson equation. HYSYS software (version 8.2) was used during the calculation of the activity coefficient.[38] The saturation pressure $P_i^{sat}$ was calculated from the Antoine equation. According to the solution-diffusion mechanism, the partial flux ($J_i$) can be written as

$$J_i = \left[\frac{P_i}{l}\right](x_i \gamma_i P_i^{sat} - y_i P^P) \tag{7}$$

where $P_i$ is the membrane permeability, $l$ is the selective layer thickness, and the term $[P_i/l]$ is known as the permeance. $y_i$ is the mole fraction of component $i$ in the permeate, and $P^P$ is the permeate pressure. The ideal membrane selectivity $\beta$ is the ratio of the permeability or permeance of two components.

## 3. RESULTS AND DISCUSSION

**3.1. Characterization of Nexar Copolymer/Ultem Composite Membranes.** Figure 2 displays the morphology

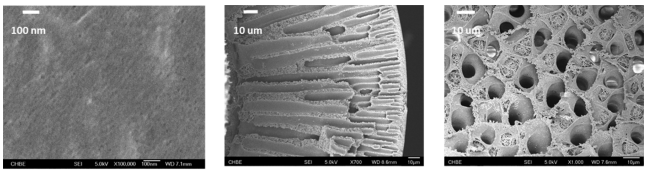


**Figure 2.** FESEM images of the Ultem hollow fiber substrates.

of the as-spun Ultem hollow fiber substrate, which is adopted from our previous study.[39] A relatively dense outer layer with no visible pores is observed under 100 000× magnification. The cross-section is fully porous with fingerlike macrovoids, and the inner surface is full of pores. This structure is purposely designed because the substrate morphology is important in the formation of composite membranes. The dense outer surface is to facilitate the deposit of the top selective layer and to prevent intrusion of the Nexar polymer during coating, while the open-pore sublayer structure provides low transport resistance and enhances the permeation rate.

Table 2 presents the dehydration performance of the Ultem substrate and some Nexar copolymer/Ultem composite membranes for an 85/15 wt % IPA/water feed mixture. The Ultem hollow fiber substrate exhibits a high permeation flux of 9.32 kg/m$^2$ h but a low separation factor of 2.8. On the other hand, after coating the Nexar copolymer on top of the substrate, the composite membranes show much enhanced separation factors up to 509 with relatively lower permeation fluxes ranging from 2.06 to 3.32 kg/m$^2$ h. This significant enhancement in separation factor results from the formation of a continuous top selective layer by means of a Nexar copolymer coating. In addition, the high permeate water concentration of above 98 wt % demonstrates the capability of the copolymer in dehydrating the IPA/water mixture. What is more, good adhesion capability or Nexar copolymer is observed when dealing with the material. It is easily adhered to polymeric substrates, such as poly(ether imide), polysulfone, poly(ether sulfone), polyacrylonitrile, and others.[26] From the FESEM image shown in Figure 3, no delamination is observed between the top selective layer and support layer. This suggests the good compatibility between the Nexar copolymer and Ultem substrate.

It is worth noting that the substrate flux is only about 3 times higher than that of the coated membrane, which reflects some support resistance of the substrate fibers. This is because the substrate has a relatively dense outer surface to provide mechanical strength and prevent intrusion during the

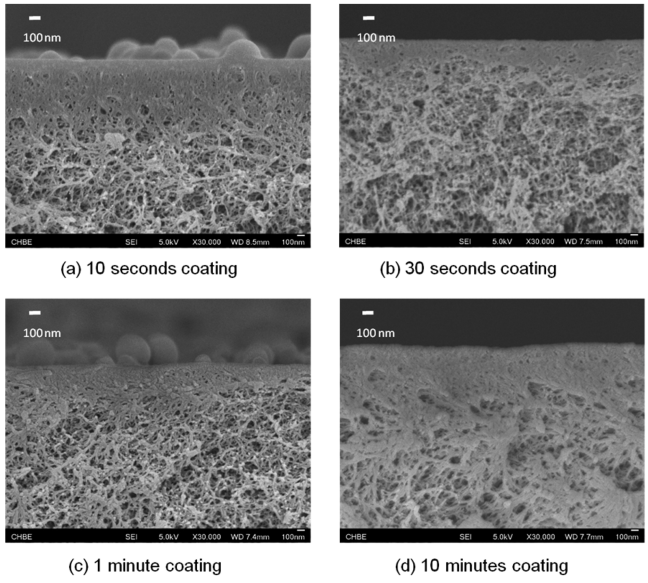


**Figure 3.** Cross-section FESEM images of the composite membranes prepared from different coating times: (a) 10 s, (b) 30 s, (c) 1 min, and (d) 10 min.

deposition of coating layer. Thus, it has some transport resistance. Nonetheless, the formed composite membranes show excellent fluxes as compared to most polymeric membranes in the literature.

For the performance assessment of pervaporation membranes, both terms of flux-separation factor and permeance selectivity can be utilized as shown in Section 2.5. The former is typically to express the operational performance of membranes, while the latter is used to show their intrinsic transport properties. Permeance is calculated from flux according to eqs 6 and 7, where the effects of driving force and operational conditions are eliminated. Selectivity is the ratio of the permeance of the two permeating components. In Table 2, since all the fibers were tested under the same operational conditions, the driving force across the membrane was not changed, and hence flux-separation factor can be used for easy comparison with literature data.

**3.2. Effect of Coating Time on the Pervaporation Performance.** To form a thin selective layer on the hollow fiber substrate via dip coating, the coating conditions play an important role on the morphology and final separation performance of the resultant composite membranes. These conditions include coating time, solution temperature, solution concentration, etc. Among them, coating time is one of the most direct parameters that affects the top layer formation.[40] Thus, its effect on pervaporation performance of the resultant membranes is investigated.

**Table 2. IPA Dehydration Performance of the Ultem® Hollow Fiber Substrate and Composite Membranes Prepared from Various Coating Time[a,b]**

| membrane | copolymer IEC value | solvent | coating time | flux (kg/m$^2$ h) | permeate water conc. (wt %) | separation factor |
|---|---|---|---|---|---|---|
| Ultem fiber | | | | 9.32 | 33.0 | 2.8 |
| Nexar/Ultem | 2.0 | hexane | 10 s | 3.32 | 85.4 | 33 |
| Nexar/Ultem | 2.0 | hexane | 30 s | 2.74 | 92.9 | 74 |
| Nexar/Ultem | 2.0 | hexane | 1 min | 2.53 | 98.1 | 293 |
| Nexar/Ultem | 2.0 | hexane | 10 min | 2.06 | 98.9 | 509 |

[a]Feed: 85/15 wt % IPA/water. [b]Operation temperature: 50 °C; downstream pressure: 1 mbar.

Table 3. IPA Dehydration Performance of the Composite Membranes Prepared from Different Solvents[a,b]

| membrane | copolymer IEC value | solvent (wt %) | coating time | flux (kg/m$^2$ h) | permeate water conc. (wt %) | separation factor |
|---|---|---|---|---|---|---|
| Nexar/Ultem | 2.0 | hexane | 30 s | 2.74 | 92.9 | 74 |
| Nexar/Ultem | 2.0 | hexane/ethanol (80/20) | 30 s | 2.35 | 98.9 | 509 |
| Nexar/Ultem | 2.0 | hexane/ethanol (70/30) | 30 s | 2.35 | 98.5 | 372 |

[a]Feed: 85/15 wt % IPA/water. [b]Operation temperature: 50 °C; downstream pressure: 1 mbar.

As tabulated in Table 2, when the coating time of the Ultem substrate in the Nexar solution is 10 s, the permeate water concentration of the resultant membrane is only 85.4 wt %. This is because either the selective layer is too thin or it cannot cover the whole substrate surface during this short coating period. Too thin a selective layer is susceptible to damage and swelling, while a defective top layer could not achieve good separation performance. Therefore, a minimum coating time of 30 s is needed to form a continuous and less defective top selective layer in this case. With the increase of coating time from 10 s to 10 min, the permeation flux decreases, while the separation factor increases. These changes are reasonable since a longer immersion time would facilitate a higher amount of the copolymer being deposited on the substrate, resulting in a thicker Nexar copolymer layer. As displayed in Figure 3, the top selective layer for the composite membrane is increased with increasing coating duration. The estimated selective layer thicknesses for the four conditions are 100, 128, 186, and 280 nm, respectively. Thus, the separation factor is improved, while the permeation flux is sacrificed correspondingly. The change in separation factor is mainly contributed by the increased thickness in selective layer. A higher thickness would result in a more tortuous path for the permeate molecules. Since IPA has a larger size than water, the tortuosity will have a larger effect on IPA permeance. Overall, an optimal coating time range of 30 s to 10 min is recommended.

From Table 2, a coating time of 1 min is the optimal condition and shows the best combined performance. However, other than searching for the best performance, this study also investigates other factors affecting the morphology and formation of the copolymer layer. A coating time of 30 s is chosen in the following sections to magnify the performance difference for membranes prepared from different conditions.

**3.3. Effect of Mixed Solvents for Nexar Copolymer on the Pervaporation Performance.** Since the Nexar pentablock copolymer is comprised of hydrophobic and hydrophilic segments, it may form different microdomain segregations under different solvents. In this work, three different solvent systems, namely, (a) hexane, (b) hexane/ethanol 80/20 wt/wt mixture, and (c) hexane/ethanol 70/30 wt/wt mixture, were used to investigate the microstructure alterations in the copolymer. The highest ethanol content of 30 wt % was chosen in the mixed solvent because of solubility limitation of the copolymer.

Table 3 lists the IPA dehydration performance of the composite membranes prepared from different solvents. With ethanol addition in the solvent, both resultant composite membranes have higher separation factors and lower fluxes as compared to the one prepared from hexane alone. This can probably be attributed to two factors associated with the inclusion of ethanol. First, ethanol can swell the hollow fiber substrate to a certain degree during the dip-coating process. Thus, a higher amount of the copolymer may be absorbed evenly on the surface and lead to the formation of a smooth and dense top layer. Second, the addition of ethanol may swell the core of the formed copolymer micelles in hexane solutions.[31] This phenomenon would increase the viscosity of the solution, which leads to a coating layer with a higher density and lower fractional free volume. According to the Choi et al. study,[29] the addition of ethanol in the pentablock copolymer can increase the solution viscosity to 3-fold. Therefore, combining the two effects, the resultant composite membranes have a smoother top layer and lower fractional free volume. Thus, an increase in separation factor but decrease in permeation flux is observed.

To confirm the above hypotheses, PAS measurements for the fractional free volume of the selective layer were carried out. Figure 4 shows the PAS spectra, where the *S* parameter is plotted as a function of positron incident energy. As the incident energy determines the penetration depth of positron into the membrane surface, the free volume at each cross section of the membrane can theoretically be exported. The graph of *S* parameter can be divided into four regions along with increasing positron incident energy. For all three membranes, there is a rapid increase of *S* parameter near the surface. This initial slope region is the first region, which is due to the back diffusion and scattering of positronium. This region is therefore normally neglected.[41] With a further increase in incident energy, *S* parameter reaches the maximum value and then gradually decreases to a flat region. These variations of *S* parameter signify the multilayer structure of the composite membranes.[42] The maximum *S* parameter region is the second region, which represents the top selective layer. The third region is the decreasing of *S* parameter until the flat region that shows the transition section from the top selective layer to the Ultem substrate. Lastly, the fourth region is the flat region of *S* parameter, which is due to the poly(ether imide) substrate material. The selective layer thickness could be estimated from the following equation:

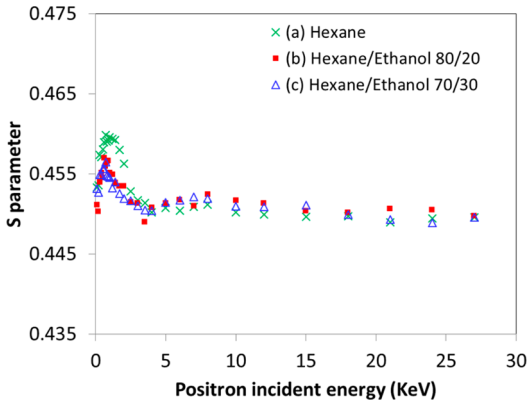


**Figure 4.** *S* parameters of the composite membranes made from different solvents: (a) hexane, (b) hexane/ethanol 80/20 wt/wt, and (c) hexane/ethanol 70/30 wt/wt.

Table 4. IPA Dehydration Performance of the Composite Membranes Prepared from Different Copolymer IEC Values[a,b]

| membrane | copolymer IEC value | solvent | coating time | water contact angle (deg) | flux (kg/m$^2$ h) | permeate water conc. (wt %) | separation factor |
|---|---|---|---|---|---|---|---|
| Nexar/Ultem | 2.0 | hexane | 30 s | 97.8 | 2.74 | 92.9 | 74 |
| Nexar/Ultem | 1.5 | hexane | 30 s | 107.7 | 2.62 | 95.2 | 112 |
| Nexar/Ultem | 1.0 | hexane | 30 s | 118.4 | 2.44 | 97.5 | 221 |

[a]Feed: 85/15 wt % IPA/water. [b]Operation temperature: 50 °C; downstream pressure: 1 mbar.

$$Z(E_+) = \left(\frac{40}{\rho}\right) E_+^{1.6} \quad (8)$$

where $Z$ is the thickness (in nanometers) at a position incident energy $E_+$ (keV), $\rho$ is the density in g/cm$^3$. The calculated top layer thickness for the membrane prepared from hexane at the maximum $S$ parameter is about 93 nm. These data are in line with those from the FESEM image, which are about 100 nm. The comparison confirms the claim that the maximum $S$ parameter is at the top selective layer.

Since the free volume of the selective layer is the interest of study, the representative $S$ parameters of the membranes are compared. As shown in Figure 4, the composite membrane prepared from hexane has a larger maximum $S$ parameter compared to the other two prepared from mixed solvents. Therefore, the former has a higher free volume and permeation flux but a lower separation factor than the latter.[43] The PAS results align well with the pervaporation performance and our hypotheses. As for the membranes prepared from solvent mixtures with 20 or 30 wt % ethanol content, the membrane morphology and density may not be changed much because of the small difference in ethanol amount. This is also reflected in the PAS spectra, where the maximum $S$ parameters for the two cases are similar, suggesting a comparable fractional free volume. Thus, these two composite membranes show similar flux and permeate water concentration.

Although the $S$ parameter is a combined measure of free volume hole size and its intensity, it is adequate to provide explanations to the observations.[41] In this case, the changes in the membranes are caused by the changes in chain packing density. So, either a reduction in hole size or number of pores would lead to a reduced fractional free volume and a smaller $S$ parameter. This change is also reflected in the pervaporation performance as discussed earlier. Therefore, the $S$ parameter is sufficient to provide the necessary information, and it is not essential to obtain the hole size and its intensity separately.

**3.4. Effect of Nexar Copolymer IEC Values on the Pervaporation Performance.** The IEC value of the copolymer is determined by the degree of sulfonation, which may change the hydrophilicity of the resultant membranes and affect the pervaporation performance. Additionally, the degree of sulfonation may alter the compatibility of the hydrophilic sulfonated fragment and other hydrophobic segments in the pentablock copolymer. As a result, the micelle structure of the copolymer in solvent is changed, and the formation of the composite membranes is influenced.

Table 4 tabulates the pervaporation data of the composite membranes prepared from copolymers with IEC values of 1.0, 1.5, and 2.0 for IPA dehydration. The permeation flux has an increasing trend when the IEC value increases from 1.0 to 2.0, while the separation factor shows the opposite. This increasing trend of flux may be explained by the increased membrane hydrophilicity at a higher IEC value. A higher hydrophilicity means a better affinity between the membrane and water molecules, which is favorable for water sorption and results in a higher permeation flux. To show the change of hydrophilicity, water contact angles of the three membranes were measured as listed in Table 4. The advancing water contact angle for the membrane with an IEC value of 1.0 is 118.4°. This represents a hydrophobic membrane surface, which is ascribed to the *t*BS and EP blocks of the copolymer. As expected, the contact angle decreases with an increase in IEC value due to the increased degree of sulfonation, reflecting the increased hydrophilicity. However, a higher hydrophilicity may cause a larger membrane swelling during pervaporation and lead to a lower separation factor.[44]

Other than the change in hydrophilicity, the alteration in micelle structure with IEC value may be another reason that affects the pervaporation performance. As depicted in Figure 5,

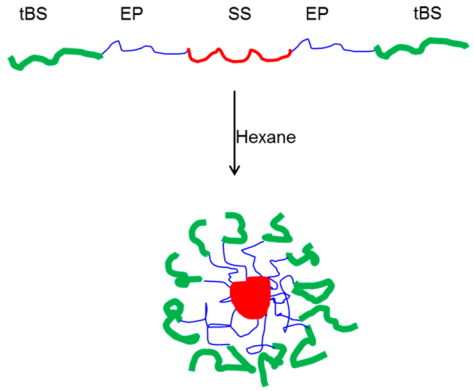


**Figure 5.** Transformation of the pentablock copolymer into a micelle structure in the hexane solvent.

the pentablock copolymer assembles itself into a micelle structure with the sulfonated segment as the core in the hexane solution.[29] Because the micelle core contains the charged group ($-SO_3$), the electron densities between the core and the shell are different. Eisenberg and his co-workers have made use of this charge contrast to study the micelle size.[45,46] They observed that the core size tends to increase with increasing degree of sulfonation because of strong incompatibility between the ionic and nonionic blocks. Therefore, maximizing the core size would help to reduce the surface energy. Similarly, when the IEC value increases from 1.0 to 2.0, the micelle size will increase to minimize the unfavorable interactions. As a result, the polymer chains would have a more stretched conformation. Additionally, the packing density of the copolymer would be reduced because of the enlarged micelle size and the resultant selective layer may have a larger fractional free volume. This may lead to an increasing flux and a decreasing separation factor for composite membranes made from higher IEC values.

To verify the structural changes in the resultant composite membranes, X-ray diffraction (XRD) and PAS techniques were utilized. Figure 6 shows the XRD spectra and the *d*-space values as calculated according to eq 1. The composite membrane prepared from IEC 2.0 possesses a diffraction peak at around

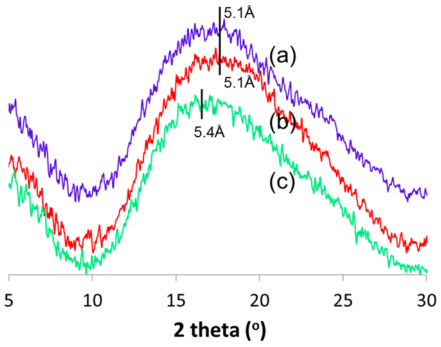


**Figure 6.** XRD curves of the composite membranes prepared from different copolymer IEC values: (a) 1.0, (b) 1.5, and (c) 2.0.

16.4° and a *d*-space value of 5.4 Å. Decreasing the IEC value to 1.5 and 1.0 shifts the diffraction peak to a higher Bragg angle that corresponds to a *d*-space value of 5.1 Å. This reduced *d*-space indicates a smaller chain−chain distance, which confirms our aforementioned explanation. Nonetheless, no obvious difference is observed between the peaks of the composite membranes made from IEC values of 1.5 and 1.0. This is probably due to the equipment sensitivity, which is unable to differentiate the small changes.

To further validate the changes in packing density of the selective layer, PAS measurements were carried out. Figure 7

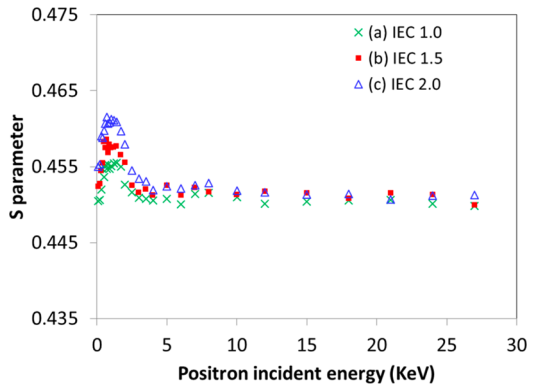


**Figure 7.** *S* parameters of the composite membranes prepared from different copolymer IEC values: (a) 1.0, (b) 1.5, and (c) 2.0.

shows the change of *S* parameter for the membranes prepared from the three IEC values. The maximum *S* parameter of each curve reflects the changes in fractional free volume of the top selective layer. An increase in IEC value results in membranes with a higher *S* parameter in the selective layer, which suggests a higher fractional free volume. These results are consistent with XRD measurements and the pervaporation performance.

**3.5. The Dehydration Performance of Nexar Copolymer/Ultem Composite Membranes for C2−C4 Alcohols.** Table 5 tabulates the pervaporation performance of the Nexar copolymer/Ultem composite membranes for dehydration of ethanol, IPA, and *n*-butanol. Impressive separation performance is achieved for IPA and *n*-butanol aqueous systems. However, the separation factor for ethanol is low, which is probably due to the effects of ethanol induced swelling to the membranes. Figure 8 compares the rate and degree of alcohol sorption by

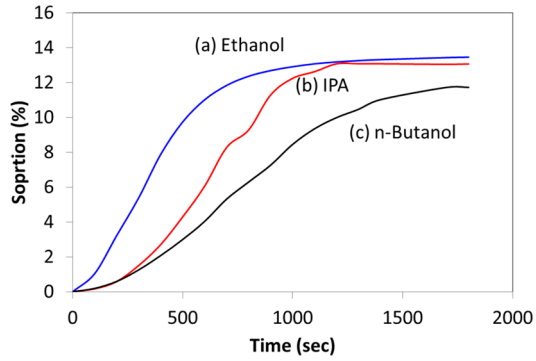


**Figure 8.** Vapor sorption results of Nexar films in various alcohols: (a) ethanol, (b) IPA, and (c) *n*-butanol.

the Nexar films. Ethanol shows the fastest sorption rate and the highest sorption extent, followed by IPA and *n*-butanol. This indicates that ethanol induces a higher swelling in the selective layer than it does in others. In addition, the swelling test results show that the degrees of membrane extension in ethanol, IPA, and *n*-butanol are 69%, 29%, and 17%, respectively. The trend aligns well with the vapor sorption data. As a consequence, ethanol dehydration has the lowest separation factor. To compare the separation factor of IPA and *n*-butanol systems, the former has a higher separation factor than the latter in spite of a smaller molecule size. This observation is consistent with many other reports in the literature.[47,48] Since penetrant linearity also plays an important role in determining the separation performance, *n*-butanol transports faster than IPA. On the other hand, because IPA has a branched structure, IPA dehydration has a higher separation factor than *n*-butanol dehydration.

Table 5 shows the order of permeation flux as such: *n*-butanol > ethanol > IPA. The same order has also been observed by Scharnagl et al.[49] To understand why the *n*-butanol/water system has the largest flux, the driving forces of water in all three systems are calculated. As shown in Table 6, both water activity coefficient and fugacity of the *n*-butanol/water system are larger than the others. This signifies the highest driving force of water across the membrane in the *n*-butanol/water system, which leads to the largest permeation flux. However, for the case of ethanol and IPA systems, the flux does not follow the order of water fugacity. This is probably due to the higher ethanol-induced membrane swelling so that the ethanol system shows a larger flux than the IPA system.[49]

**Table 5. Dehydration Performance of the Composite Membranes for C2−C4 Alcohols[a,b]**

| alcohol | copolymer IEC value | solvent | coating time | flux (kg/m$^2$ h) | permeate water conc. (wt %) | separation factor |
|---|---|---|---|---|---|---|
| ethanol | 2.0 | hexane | 10 min | 2.30 | 79.5 | 23 |
| IPA | 2.0 | hexane | 10 min | 2.06 | 98.9 | 509 |
| *n*-butanol | 2.0 | hexane | 10 min | 2.46 | 97.4 | 212 |

[a]Feed: 85/15 wt % alcohol/water. [b]Operation temperature: 50 °C; downstream pressure: 1 mbar.

**Table 6. Comparison of Fugacity and Permeance[a,b] of the Three Alcohol Systems**

| alcohol | water activity coefficient | water $P^{sat}$ (kPa) | water fugacity (kPa) | water permeance (GPU)[c] | alcohol permeance (GPU) |
|---|---|---|---|---|---|
| ethanol | 1.92 | 12.31 | 6.99 | 12 050 | 375 |
| IPA | 2.04 | 12.31 | 9.31 | 10 090 | 18 |
| *n*-butanol | 2.12 | 12.31 | 10.98 | 10 070 | 205 |

[a]Feed: 85/15 wt % alcohol/water. [b]Operation temperature: 50 °C; downstream pressure: 1 mbar. [c]1 GUP = $1 \times 10^{-6}$ $cm^3$ (STP)/$cm^2$ s cmHg.

To decouple the effect of driving force and further inspect the separation performance, the flux is converted to permeance as listed in Table 6. The water permeance shows a deceasing order from C2 to C4 alcohols, which follows the trend of swelling tendency induced by alcohols on membranes. The higher the swelling, the larger the amount of water that may pass through the membrane when the driving force is normalized. On the other hand, the alcohol permeance has an order of ethanol > *n*-butanol > IPA. This result can probably be explained by the size and linearity of the alcohol molecules, where ethanol is small and IPA has a branch. However, for a more comprehensive comparison, the complicated interactions among water, alcohol, and the membrane should also be considered,[50,51] which is not the focus of this study.

In summary, the newly developed Nexar copolymer/Ultem composite membranes show impressive dehydration performance for IPA and *n*-butanol, which is probably because the block copolymer effectively synergizes the advantages of different chemical structures. The composite membrane also shows good stability within the pervaporation testing time of 1 d. However, since the lab-scale setup is not designed to run in a continuous mode, and the number of our lab-scale setups is limited, it is difficult for us to occupy a setup for a single test for a long time. Therefore, the purpose in this work is to demonstrate the feasibility of the membrane only. The long-term stability issue may be addressed in future works. Figure 9

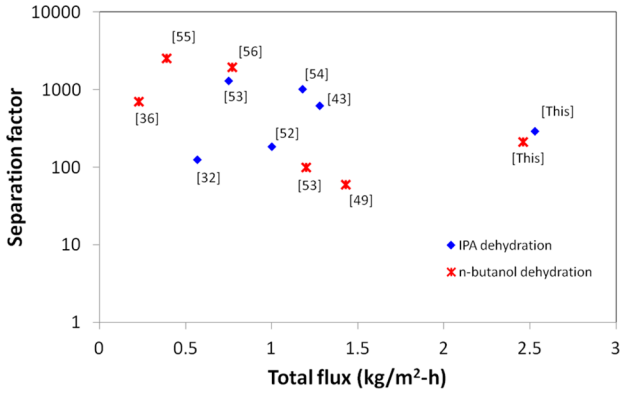


**Figure 9.** A comparison of polymeric membranes for pervaporation dehydration of IPA and *n*-butanol.

compares the dehydration performance between the current work and literature data.[32,36,43,49,52−56] The newly developed composite membranes show superior fluxes with better separation factors than most other polymeric membranes. The study may provide useful guidelines and insights in designing and applying block copolymers for pervaporation applications.

## 4. CONCLUSIONS

In this work, novel composite membranes comprising Nexar block copolymers as the selective layer have been developed for pervaporation dehydration of C2−C4 alcohols. In-depth investigations on the physicochemical properties, morphologies, and separation performance of the composite membranes were carried out. The following conclusions can be drawn from the current study:

(1) By using a dip-coating method, the copolymer was successfully deposited on the Ultem hollow fiber substrate. A minimum coating time of 30 s is needed for the formation of a continuous and less defective selective layer. The resultant membranes show a flux decrease and a separation factor increase with an increase in coating time because of forming a thicker top selective layer.

(2) The effects of different solvent systems on the formation of composite membranes were investigated. With the addition of ethanol as a cosolvent for the copolymer, the resultant membranes exhibit a higher separation factor but a lower flux than the one using hexane as the solvent. This could be attributed to (1) the ethanol-induced substrate swelling and (2) the ethanol-induced swelling of micelle core of the copolymer. Both effects help the formation of a smooth and dense selective layer, which have been verified by PAS measurements.

(3) The IEC value of the Nexar polymer affects the pervaporation performance of the resultant membranes. The higher the IEC value, the larger the permeation flux and the smaller the separation factor. This is ascribed to the change in polymer hydrophilicity and alternation in polymer chain conformation.

(4) The newly developed composite membranes demonstrate good separation performance for IPA and *n*-butanol dehydration with fluxes exceeding 2 $kg/m^2$ h and separation factors of more than 200. The performance for ethanol dehydration may need improvements in future studies.

## AUTHOR INFORMATION

### Corresponding Author

*E-mail address: chencts@nus.edu.sg. Phone: 65 6516 6645. Fax: 65 6779 1936.

### Notes

The authors declare no competing financial interest.

## ACKNOWLEDGMENTS

The authors thank the National Research Foundation, Prime Minister's Office, Singapore under its Competitive Research Program (CRP Award No. NRF-CRP 5-2009-5 (NUS Grant No. R-279-000-311-281)) for funding this research. We would also gratefully thank Kraton Polymer Inc. for their support under the project entitled "Evaluation of Nexar Polymers for Water Filtration Applications" (Grant No. R-279-000-396-597). Thanks are due to Dr. C. L. Willis for his kind support and help.

## REFERENCES

(1) Feng, X. S.; Huang, R. Y. M. Preparation and Performance of Asymmetric Polyetherimide Membranes for Isopropanol Dehydration by Pervaporation. *J. Membr. Sci.* **1996**, *109*, 165−172.

(2) Vane, L. M. A Review of Pervaporation for Product Recovery from Biomass Fermentation Processes. *J. Chem. Technol. Biotechnol.* **2005**, *80*, 603−629.
(3) Huang, Y.; Baker, R. W.; Wijmans, J. G. Perfluoro-Coated Hydrophilic Membranes with Improved Selectivity. *Ind. Eng. Chem. Res.* **2013**, *52*, 1141−1149.
(4) Jiang, L. Y.; Wang, Y.; Chung, T. S.; Qiao, X. Y.; Lai, J. Y. Polyimides MMembranes for Pervaporation and Biofuels Separation. *Prog. Polym. Sci.* **2009**, *34*, 1135−1160.
(5) Zuo, J.; Chung, T. S. Design and Synthesis of a Fluoro-Silane Amine Monomer for Novel Thin Film Composite Membranes to Dehydrate Ethanol via Pervaporation. *J. Mater. Chem. A* **2013**, *1*, 9814−9826.
(6) Hung, W. S.; An, Q. F.; Guzman, De M.; Lin, H. Y.; Huang, S. H.; Liu, W. R.; Hu, C. C.; Lee, K. R.; Lai, J. Y. Pressure-Assisted Self-Assembly Technique for Fabricating Composite Membranes Consisting of Highly Ordered Selective Laminate Layers of Amphiphilic Graphene Oxide. *Carbon* **2014**, *68*, 670−677.
(7) Chapman, P. D.; Oliveria, T.; Livingston, A. G.; Li, K. Membranes for the Dehydration of Solvents by Pervaporation. *J. Membr. Sci.* **2008**, *318*, 5−37.
(8) Shao, P.; Huang, R. Y. M. Polymeric Membrane Pervaporation. *J. Membr. Sci.* **2008**, *287*, 162−179.
(9) Bolto, B.; Hoang, M.; Xie, Z. A Review of Membrane Selection for the Dehydration of Aqueous Ethanol by Pervaporation. *Chem. Eng. Process.* **2011**, *50*, 227−235.
(10) Le, N. L.; Wang, Y.; Chung, T. S. Synthesis, Cross-Linking Modification of 6FDA-NDA/DABA Polyimide Membranes for Ethanol Dehydration via Pervaporation. *J. Membr. Sci.* **2012**, *415*−*416*, 109−121.
(11) Wang, Y.; Goh, S. H.; Chung, T. S. Miscibility Study of Torlon® Polyamide-imide with Matrimid® 5218 Polyimide and Polybenzimidazole. *Polymer* **2007**, *48*, 2901−2909.
(12) Yoshikawa, M.; Higuchi, A.; Ishikawa, M.; Guiver, M. D.; Robertson, G. P. Vapor Permeation of Aqueous 2-propanol Solutions Through Gelatin/Torlon® Poly(amide imide) Blended Membranes. *J. Membr. Sci.* **2004**, *243*, 89−95.
(13) Higuchi, A.; Yoshikawa, M.; Guiver, M. D.; Robertson, G. P. Vapor Permeation and Pervaporation of Aqueous 2-propanol Solutions Through the Torlon® Poly(amide imide) Membranes. *Sep. Sci. Technol.* **2005**, *40*, 2697−2707.
(14) Liu, Y. L.; Hsu, C. Y.; Su, Y. H.; Lai, J. Y. Chitosan-Silica Complex Membranes from Sulfonic Acid Functionalized Silica Nanoparticles for Pervaporation Dehydration of Ethanol−Water Solutions. *Biomacromolecules* **2005**, *6*, 368−373.
(15) Chang, B. J.; Chang, Y. H.; Kim, D. K.; Kin, J. H.; Lee, S. B. New Copolyimide Membranes for the Pervaporation of Trichloroethylene from Water. *J. Membr. Sci.* **2005**, *248*, 99−107.
(16) Nunes, S. P.; Car, A. From Charge-Mosaic to Micelle Self-Assembly: Block Copolymer Membranes in the Last 40 Years. *Ind. Eng. Chem. Res.* **2013**, *52*, 993−1003.
(17) Odani, H.; Taira, K.; Nemoto, N.; Kurata, M. Permeation and Diffusion of Gases in Styrene-Butadiene-Styrene Block Copolymers. *Bull. Inst. Chem. Res., Kyoto Univ.* **1975**, *53*, 216−248.
(18) Boddeker, D. Pervaporation of Phenols, European Patent (EP) 0,264,113, 1988.
(19) Boddeker, K. W.; Bengtson, G.; Pingel, H. Pervaporation of Isomeric Butanols. *J. Membr. Sci.* **1990**, *54*, 1.
(20) Buonomenna, M. G.; Golemme, G.; Tone, C. M.; Santo, De M.P.; Ciuchi, F.; Perrotta, E.; Zappone, B.; Galiano, F.; Figoli, A. Ordering Phenomena in Nanostructured Poly(styrene-b-butadiene-b-styrene) (SBS) Membranes for Selective Ethanol Transport. *J. Membr. Sci.* **2011**, *385*−*386*, 162−170.
(21) Kuila, S. B.; Ray, S. K. Dehydration of Acetic Acid by Pervaporation Using Filled IPN Membranes. *Sep. Purif. Technol.* **2011**, *81*, 295−306.
(22) Ray, S.; Ray, S. K. Synthesis of Highly Selective Copolymer Membranes and Their Application for the Dehydration of Tetrahydrofuran by Pervaporation. *J. Appl. Polym. Sci.* **2007**, *103*, 728−737.
(23) Kuila, S. B.; Ray, S. K. Separation of Isopropyl Alcohol−Water Mixtures by Pervaporation Using Copolymer Membrane: Analysis of Sorption and Permeation. *Chem. Eng. Res. Des.* **2013**, *91*, 377−388.
(24) Mandal, S.; Pangarkar, V. G. Pervaporation Dehydration of 1-Methoxy Propanol with Acrylonitrile-Based Copolymer Membranes Prepared Through Emulsion Polymerization: A Solubility Parameter Approach and Study of Structural Impact. *J. Membr. Sci.* **2002**, *209*, 53−66.
(25) Geise, G. M.; Freeman, B. D.; Paul, D. R. Characterization of a Sulfonated Pentablock Copolymer for Desalination Applications. *Polymer* **2010**, *51*, 5815−5822.
(26) Duong, P. H. H.; Chung, T. S.; Wei, S.; Irish, L. Highly Permeable Double-Skinned Forward Osmosis Membranes for Anti-Fouling in the Emulsified Oil−Water Separation Process. *Environ. Sci. Technol.* **2014**, *48*, 4537−4545.
(27) Willis, C. L.; Handlin Jr., D. L.; Trenor, S. R.; Mather, B. D. Sulfonated Block Copolymers, Method for Making Same, and Various Uses for Such Block Copolymers, U.S. Patent 7,737,224, 2010.
(28) Choi, J. H.; Willis, C. L.; Winey, K. I. Effects of Neutralization with Et3Al on Structure and Properties in Sulfonated Styrenic Pentablock Copolymers. *J. Membr. Sci.* **2013**, *428*, 516−522.
(29) Choi, J. H.; Kora, A.; Winey, K. I. Micellar Morphology in Sulfonated Pentablock Copolymer Solutions. *Ind. Eng. Chem. Res.* **2010**, *49*, 12093−12097.
(30) Gao, R.; Wang, D.; Heflin, J. R.; Long, T. E. Imidazolium Sulfonate-Containing Pentablock Copolymer-Ionic Liquid Membranes for Electroactive Actuators. *J. Mater. Chem.* **2012**, *22*, 13473−13476.
(31) Choi, J. H.; Willis, C. L.; Winey, K. I. Structure-Property Relationship in Sulfonated Pentablock Copolymers. *J. Membr. Sci.* **2012**, *394*, 169−174.
(32) Liu, R. X.; Qiao, X. Y.; Chung, T. S. Dual-Layer P84/Polyethersulfone Hollow Fiber for Pervaporation Dehydration of Isopropanol. *J. Membr. Sci.* **2007**, *294*, 103−114.
(33) Zuo, J.; Wang, Y.; Chung, T. S. Novel Organic-Inorganic Thin Film Composite Membranes with Separation Performance Surpassing Ceramic Membranes for Isopropanol Dehydration. *J. Membr. Sci.* **2013**, *433*, 60−71.
(34) Chen, H. M.; Hung, W. S.; Lo, C. H.; Huang, S. H.; Cheng, M. L.; Liu, G.; Lee, K. R.; Lai, J. Y.; Sun, Y. M.; Hu, C. C.; Suzuki, R.; Ohdaira, T.; Oshima, N.; Jean, Y. C. Free-Volume Depth Profile of Polymeric Membranes Studied by Positron Annihilation Spectroscopy: Layer Structure from Interfacial Polymerization. *Macromolecules* **2007**, *40*, 7542−7557.
(35) Li, F. Y.; Li, Y.; Chung, T. S.; Chen, H. M.; Jean, Y. C.; Kawi, S. Development and Positron Annihilation Spectroscopy (PAS) Characterization of Polyamide Imide (PAI)-Polyethersulfone (PES) Based Defect-Free Dual-Layer Hollow Fiber Membranes with Ultrathin Dense-Selective Layer for Gas Separation. *J. Membr. Sci.* **2011**, *378*, 541−550.
(36) Shi, G. M.; Yang, T. X.; Chung, T. S. Polybenzimidazole (PBI)/Zeolitic Imidazolate Frameworks (ZIF-8) Mixed Matrix Membranes for Pervaporation Dehydration of Alcohols. *J. Membr. Sci.* **2012**, *415*−*416*, 577−586.
(37) Jiang, L. Y.; Chen, H. M.; Jean, Y. C.; Chung, T. S. Ultrathin Polymeric Interpenetration Network with Separation Performance Approaching Ceramic Membranes for Biofuel. *AIChE J.* **2009**, *55* (1), 75−86.
(38) Wang, Y.; Jiang, L. Y.; Matsuura, T.; Chung, T. S.; Goh, S. H. Investigation of the Fundamental Differences between Polyamide-imide (PAI) and Polyetherimide (PEI) Membranes for Isopropanol Dehydration via Pervaporation. *J. Membr. Sci.* **2008**, *318*, 217−226.
(39) Zuo, J.; Lai, J. Y.; Chung, T. S. In-situ Synthesis and Cross-Linking of Polyamide Thin Film Composite (TFC) Membranes for Bioethanol Applications. *J. Membr. Sci.* **2014**, *458*, 47−57.
(40) Xiangli, F.; Wei, W.; Chen, Y.; Jin, W.; Xu, N. Optimization of Preparation Conditions for Polydimethylsiloxane (PDMS)/Ceramic

Composite Pervaporation Membranes Using Response Surface Methodology. *J. Membr. Sci.* **2008**, *311*, 23−33.
(41) Huang, S. H.; Huang, W. S.; Liaw, D. J.; Lo, C. H.; Chao, W. C.; Hu, C. C.; Li, C. L.; Lee, K. R.; Lai, J. Y. Interfacially Polymerized Thin-Film Composite Polyamide Membranes: Effects of Annealing Processes on Pervaporation Dehydration of Aqueous Alcohol Solutions. *Sep. Purif. Technol.* **2010**, *72*, 40−47.
(42) Chao, W. C.; Huang, S. H.; An, Q. F.; Liaw, D. J.; Huang, Y. C.; Lee, K. R.; Lai, J. Y. Novel Interfacially-Polymerized Polyamide Thin-Film Composite Membranes: Studies on Characterization, Pervaporation, and Positron Annihilation. *Polymer* **2011**, *52*, 2414−2421.
(43) Zuo, J.; Wang, Y.; Sun, S. P.; Chung, T. S. Molecular Design of Thin-Film Composite (TFC) Hollow Fiber Membranes for Isopropanol Dehydration via Pervaporation. *J. Membr. Sci.* **2012**, *405*−*406*, 123−133.
(44) Feng, X. S.; Huang, R. Y. M. Liquid Separation by Membrane Pervaporation: A Review. *Ind. Eng. Chem. Res.* **1997**, *36*, 1048−1066.
(45) Nguyen, D.; Varsheny, S. K.; Williams, C. E.; Eisenberg, A. Micellar Morphology in Bulk Styrene-Core Ionic Diblock Copolymers. *Macromolecules* **1994**, *27*, 5086−5089.
(46) Nguyen, D.; Zhong, X. F.; Williams, C. E.; Eisenberg, A. Effect of Ionic Chain Polydispersity on the Size of Spherical Ionic Microdomains in Diblock Ionomers. *Macromolecules* **1994**, *27*, 5173−5181.
(47) Jiang, L. Y.; Chung, T. S.; Rajagopalan, R. Dehydration of Alcohols by Pervaporation through Polyimide Matrimid® Asymmetric Hollow Fibers with Various Modification. *Chem. Eng. Sci.* **2008**, *63*, 204−216.
(48) Lee, Y. M.; Nam, S. Y.; Ha, S. Y. Pervaporation of Water/Isopropanol Mixtures through Polyaniline Membranes Doped with Poly(acrylic acid). *J. Membr. Sci.* **1999**, *159*, 41−46.
(49) Scharnagl, N.; Peinemann, K. V.; Wenzlaff, A.; Schwarz, H. H.; Behling, R. D. Dehydration of Organic Compounds with SYMPLEX Composite Membranes. *J. Membr. Sci.* **1996**, *113*, 1−5.
(50) Qiao, X.; Chung, T. S.; Guo, W. F.; Matsuura, T.; Teoh, M. M. Dehydration of Isopropanol and Its Comparison with Dehydration of Butanol Isomers from Thermodynamic and Molecular Aspects. *J. Membr. Sci.* **2005**, *252*, 37−49.
(51) Wijmans, J. G. Process Performance = Membrane Properties + Operating Conditions. *J. Membr. Sci.* **2003**, *220*, 1−3.
(52) Teoh, M. M.; Chung, T. S.; Wang, K. Y.; Guiver, M. D. Exploring Torlon/P84 Co-polyamide-imide Blended Hollow Fibers and Their Chemical Cross-Linking Modifications for Pervaporation Dehydration of Isopropanol. *Sep. Purif. Technol.* **2008**, *61*, 404−413.
(53) Liu, Y. L.; Yu, C. H.; Lee, K. R.; Lai, J. Y. Chitosan/Poly(tetrafluoroethylene) Composite Membranes Using in Pervaporation Dehydration Processes. *J. Membr. Sci.* **2007**, *287*, 230−236.
(54) Zhao, Q.; Qiao, J.; An, Q.; Sun, Z. Layer-by-Layer Self-Assembly of Polyelectrolyte Complexes and Their Multilayer Films for Pervaporation Dehydration of Isopropanol. *J. Membr. Sci.* **2010**, *346*, 335−343.
(55) Widjojo, N.; Chung, T. S. Pervaporation Dehydration of $C_2$−$C_4$ Alcohols by 6FDA-ODA-NDA/Ultem® Dual-Layer Hollow Fiber Membranes with Enhanced Separation Performance and Swelling Resistance. *Chem. Eng. J.* **2009**, *155*, 736−743.
(56) Wang, Y.; Goh, S. H.; Chung, T. S.; Peng, N. Polyamide-imide/Polyetherimide Dual-Layer Hollow Fiber Membranes for Pervaporation Dehydration of C1−C4 Alcohols. *J. Membr. Sci.* **2009**, *326*, 222−233.